Journal of Interfaces, Thin films, and Low dimensional systems 3 (1) Summer and Autumn (2019) 211-218
Archive of SID

Synthesis of crystalline Tellurium nanowires by thin film fabrication via thermal evaporation method

Scientific research paper

Nahid Parsafar* and Akbar Ebrahimzad

Research Institute of Applied Sciences, Academic Center of Education, Culture and Research (ACECR), Shahid Beheshti University, Tehran, Iran

ARTICLE INFO

Article history:
Received 24 November 2019
Revised 14 February 2020
Accepted 17 May 2020
Available online 12 June 2020

Keywords:
Tellurium
Nanowire
Thermal evaporation
Tube furnace

ABSTRACT

Tellurium nanostructures have attracted much interest due to their interesting properties such as gas sensing, photoconductivity, nonlinear optical response, and high thermoelectric or piezoelectric responses. Crystalline Tellurium nanowires were successfully synthesized at 10^{-1} mbar, 10^{-2} mbar, and 10^{-3} mbar pressures by thin film fabrication via evaporation of Tellurium powder and its condensation on glass substrates at different temperatures in a tube furnace. The morphology and size of the products were studied using field emission scanning electron microscopy (FESEM). The synthesized nanowires have diameters between 46 and 100 nm and lengths up to several micrometers. X-Ray diffractometry (XRD) was carried out to characterize crystal structure of the products. The peaks of the diffractogram were successfully indexed assuming the hexagonal crystal structure of Tellurium.

1 Introduction

Tellurium (Te) is a rare element with abundance in the Earth's crust of 1 ppb. Its melting and boiling points are 449.5°C and 988°C respectively. Tellurium in the bulk form is a p-type narrow band gap (0.33 eV) semiconductor at room temperature [1]. Tellurium has a crystalline structure with high anisotropy, with the basic unit being helical chains of covalently bound Te atoms. These chains are connected together to form a hexagonal lattice through weaker Van der Waals forces. Such an inherently anisotropic structure tends to grow along the [0 0 0 1] direction [2, 3].

As an important semiconductor, Tellurium has attracted much interest due to its unusual anisotropic crystal structure and useful properties. Tellurium nanostructures show interesting properties such as gas sensing [4, 5], unique photoconductivity, nonlinear optical response, and high thermoelectric or piezoelectric responses [6, 7]. Ran et al. investigated the mechanical properties and piezoresistivity of Tellurium nanowires (TeNWs). He estimated the elastic modulus and observed the elastic and elastic–plastic behaviors of the nanowires and together with their piezoresistive effects [8]. Tellurium nanowires can be used in the manufacture of different nanocomposites. For example, Balguri et al. studied the flexural properties of TeNWs/epoxy nanocomposites. He observed significant enhancement in the flexural strength of TeNWs/epoxy nanocomposite in comparison to plain epoxy composites [9]. Yan et al. showed that at a low loading ratio of 2.4 vol %, TeNWs/epoxy

*Corresponding author.
Email address: Nahidparsafar@Rias.ac.ir
DOI: 10.22051/jitl.2020.29196.1035
www.SID.ir

Archive of SID

nanocomposites exhibits the out-of-plane and in-plane thermal conductivity which is 189% and 715% higher than that of pure epoxy resin, respectively. In addition, good stability and flexibility of nanocomposites are well maintained [10].

Pharmaceutical applications of TeNWs have also been recently considered. Wu et al. claimed that TeNWs with lengths below 100 nm have high stability in vivo which can selectively kill cancer cells while having negligible effects on normal cells. They stated that both in vitro and in vivo experiments indicate that TeNWs are a promising inorganic nano-prodrug that exerts good selective therapeutic effects on tumors [11]. Berezovets et al. investigated electron transport in TeNWs. Their results are in agreement with the concept regarding the major mechanism of current in a way that one-dimensional wires depend only on the dimension of conducting wires [12]. Many functional materials such as CdTe, ZnTe, Bi_2Te_3, etc., can also be synthesized by the reaction of Tellurium with other elements [13, 14].

Various methods have been developed to synthesize 1-dimensional Tellurium nanostructures, such as electrochemical and electrophoretic deposition [15], solution-phase approach [16], surfactant-assisted growth [7, 17], hydrothermal method [18, 19, 20, 21], microwave [22], and laser-assisted synthesis [23]. Zhao & Ye reported both electrochemical and electrophoretic deposition of high-density TeNWs arrays with wires of 60 nm diameter and lengths of 15–20 μm in the nanochannels of anodic aluminum oxide (AAO) templates [15]. Wang et al. synthesized single-crystalline TeNWs and nanotubes from Tellurium powder through a hydrothermal recrystallization route. They reported that the TeNWs, exhibited excellent sensitivity to NH_3 at room temperature [19]. Liang & Qian synthesized TeNWs via the hydrothermal reaction at 160 °C by using Na_2TeO_3 and $Na_2S_2O_3$ as starting materials [20]. In addition, TeNWs synthesis was carried out in the wet-chemical method at 105 °C under crowded conditions of inert macromolecules, using solutions of sodium Tellurite (Na_2TeO_3) as a precursor, hydrazine (N_2H_4) as a reducing agent, and polyvinylpyrrolidone (PVP) as both a stabilizing and crowding agent. This method was implemented by Hunyadi [24]. Li et al. prepared TeNWs through the self-seed-assisted growth method. The Tellurium seeds were firstly synthesized by reducing Na_2TeO_3 in the ice water with $NaBH_4$. Then the TeNWs were grown on Tellurium seeds by reducing Na_2TeO_3 with hydrazine hydrate [25]. Gautam & Rao synthesized the one dimensional crystalline nanostructures of Tellurium by a self-seeding solution process [26]. Silva et al. reported the synthesis of single-crystalline TeNWs with different aspect-ratios prepared via surfactant-assisted synthesis under mild conditions. Short and long TeNWs were synthesized by reduction of Tellurium dioxide by hypophosphorous acid assisted by polyoxyethylene (23) lauryl ether and cetyltrimethylammonium bromide, respectively [1].

Among the reported methods for the synthesis of 1-demensional Tellurium nanostructures, vapor-phase synthesis is of great importance [27-29]. The physical evaporation method produces very high-purity nanostructures. Sapkota et al. reported the synthesis of ultrathin Tellurium nanostructures by high temperature vapor phase deposition on c-plane sapphire substrates [30]. Parsafar & Ebrahimzad investigated effect of the substrate temperature on the formation of Tellurium nanostructures by the physical evaporation method [31].

In this work, we report the synthesis of single-crystalline TeNWs by thin film creation via a facile low temperature vaporization method. It should be mentioned that in the physical evaporation method, many different self-assembled structures of Tellurium are obtained. The characteristic of this study is to find the nanowire formation conditions at five different pressures (atmosphere, 1 mbar, 10^{-1} mbar, 10^{-2} mbar, and 10^{-3} mbar). Of course the nanowire formation was not observed at 1 mbar and atmosphere pressures in the used tube furnace.

2 Experimental setup

In this study, a horizontal tube furnace was used for physical evaporation of Tellurium. This furnace is specifically designed to provide a temperature gradient along the length of the heated zone. The main body of the furnace is made of hipped alumina ceramic in which another tube of quartz is inserted to prevent alumina contamination. The boat containing high-

www.SID.ir

Archive of SID

purity Tellurium powder (99.99%) from Merck is made of tungsten, which is placed in the middle of the hot zone of the furnace. The substrates were cleaned in an ultrasonic bath of acetone for 10 min, distilled water for 10 min and dried in hot air flow.

Table 1. Details of deposition conditions for nanowires synthesis.

Sample	Evaporation temperature (°C)	Substrate	Pressure (mbar)
1	333	Glass	10^{-1}
2	350	Glass	10^{-1}
3	360	Glass	10^{-2}
4	360	Glass	10^{-2}
5	360	Glass	10^{-2}
6	353	Glass	10^{-3}
7	353	Glass	10^{-3}
8	353	Silicon(100)	10^{-3}
9	353	Silicon(100)	10^{-3}
Sample	Substrate temperature (°C)	Substrate distance to boat (cm)	
1	132	32.5	
2	185	27.5	
3	177	29	
4	186	28	
5	196	27	
6	136	33	
7	213	24	
8	146	32	
9	235	21.5	

After cleaning, they were placed in specified locations on a ruler made of pyrex. This ruler was placed downstream of argon gas flow in the furnace. Argon gas was used to regulate the pressure inside the furnace as carrier gas. In this system the gas flow was controlled by an Apex mass flow controller. Schematic diagram of the experimental setup is shown in Figure 1.

In order to achieve the desired pressures, the chamber was initially evacuated to 10^{-3} mbar at room temperature and then was purged with argon gas and heated to the desired temperature. The pressure of 10^{-1} mbar and 10^{-2} mbar was generated by the flow of 10 sccm and 7 sccm of argon gas, respectively. In the case of 10^{-3} mbar, we did not have any gas flow. The deposition times in these experiments were 90 minutes.

In this study many experiments were performed with different conditions for the synthesis of nanostructures. At each pressure, boat temperature, and depending on the distance of substrate to boat, different structures were synthesized, such as nanotubes, nanorods, nanowires, nanobelts and so on. In the some of these conditions, nanowires were synthesized. Table 1 summarizes the conditions of all the situations in which, the nanowires were synthesized.

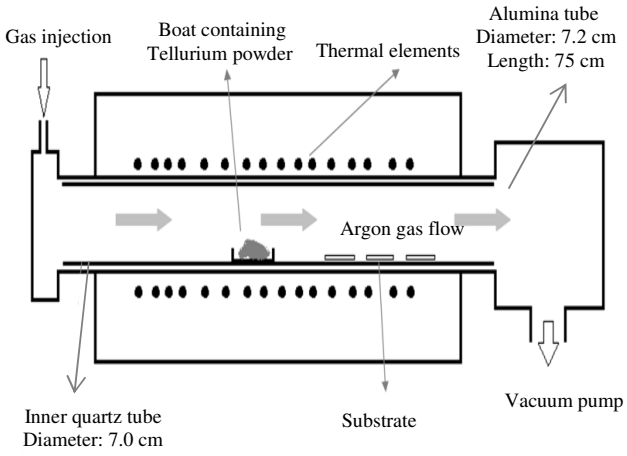

Figure 1. Schematic diagram of the tube furnace.

A Hitachi S-4160 field emission scanning electron microscope was used to obtain FESEM images and the morphology of the synthesized structures. The xrd patterns were also obtained by a D8 Advanced Bruker diffractometer (35 kV, 30 mA, monochromatic CuKα (λ=1.54 Å) radiation step size of 0.04 (2θ/S)).

www.SID.ir

Archive of SID

3 Results and discussion

As mentioned before by evaporating Tellurium at relatively low temperatures and forming thin films, we were able to synthesize high purity nanowires. Figures 2a and 2b show the FESEM images of the structures synthesized on a 132°C glass substrate placed at 32.5 cm from the boat in the downstream of argon gas flow. The temperature of the boat was 333°C at 10^{-1} mbar. As it is seen, curved nanowires have grown on the substrate surface. It is clear from the images that the length of the nanowires reach to several micrometers.

The XRD pattern of this sample, shown in Figure 3, indicates that the most intense peak is due to the reflection from (102) crystal plane. All the observed peaks in the diffractogram were indexed assuming the hexagonal crystal structure in accordance with JCPDS No. 36-1452.

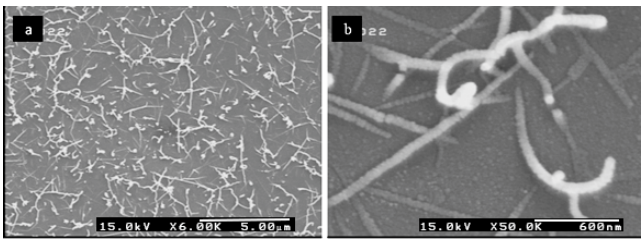

Figure 2. FESEM images of grown structures at 10^{-1} mbar pressure on a 132 °C glass substrate placed at 32.5 cm from the 333 °C boat.

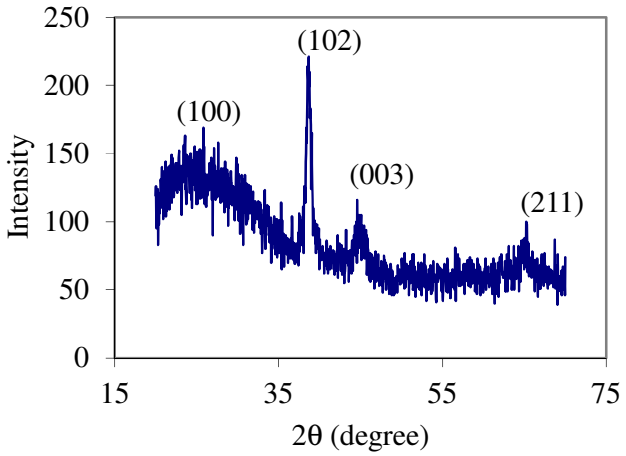

Figure 3. XRD pattern of the synthesized Tellurium nanostructures at 10^{-1} mbar pressure on a 132 °C glass substrate placed at 32.5 cm from the 333 °C boat in the downstream of argon flow.

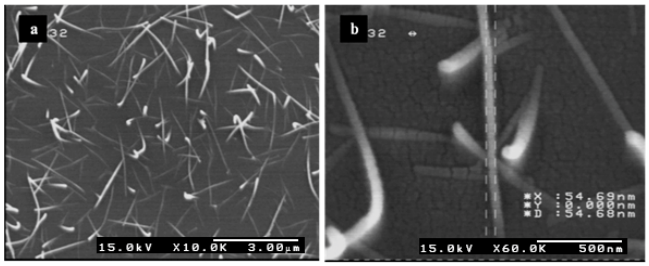

Figure 4. FESEM images of grown structures at 10^{-1} mbar pressure on 185 °C glass substrate placed at 27.5 cm from the 350 °C boat.

In the second experiment, the temperature of the boat was 350 °C while the pressure was regulated at 10^{-1} mbar. Figures 4a and 4b show the FESEM images of the structures synthesized on a 185 °C glass substrate placed at 27.5 cm from the boat in the downstream of argon gas flow. Figure 4a indicates thin and relatively long nanowires. Figure 4b shows a typical nanowire with nearly uniform diameter of 54 nm.

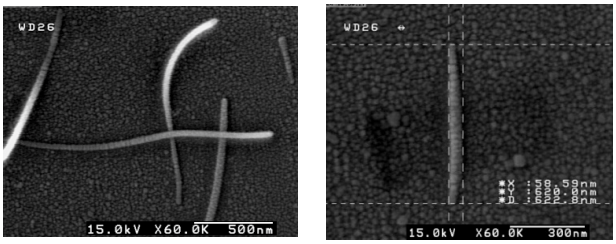

A b

Figure 5. FESEM images of grown structures at 10^{-2} mbar pressure on a 177 °C glass substrate placed at 29 cm from the 360 °C boat.

In the other experiment, the temperature of the boat was 360 °C while the pressure was regulated at 10^{-2} mbar. As shown in Figure 5a, low density nanowires were synthesized on a 177 °C glass substrate at 29 cm from the boat in the downstream of argon gas flow. In Figure 5a, we can see that most of these wires have a length more than one micrometer. Figure 5b shows one of these nanowires with a diameter of about 59 nm.

www.SID.ir

Archive of SID

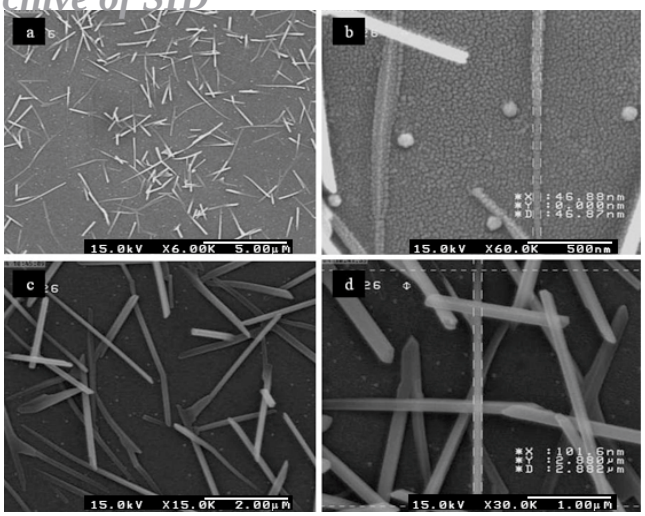

Figure 6. FESEM images of grown structures at 10^{-2} mbar pressure. Panels a and b are the images of synthesized structures on a 186 ^{o}C glass substrate placed at 28 cm from the 360 ^{o}C boat. Panels c and d are the images of synthesized structures at 10^{-2} mbar pressure on a 196 ^{o}C glass substrate placed at 27 cm from the 360 ^{o}C boat.

Figure 6a is a low magnification FESEM image of the structures synthesized at 10^{-2} mbar. These nanowires were grown on a 186 ^{o}C glass substrate placed at 28 cm from the 360 ^{o}C boat in the downstream of argon gas flow. As it is seen, the products are straight nanowires with relatively long lengths grown on the glass substrate surface. Figure 6b shows a typical nanowire synthesized in these conditions with a slightly needle-like structure. Besides TeNWs, the FESEM micrograph indicates nano-size Tellurium spheres on the surface, which seems to be nucleation sites for growth of nanowires.

Figures 6c and 6d show the structures grown on glass substrate at 27 cm from the 360 ^{o}C boat at a pressure of 10^{-2} mbar and a substrate temperature of 196^{o}C, which are mostly nanowires. Figure 6d shows one of these structures with a diameter of about 100 nm. The increase in diameter of the synthesized nanostructure is due to the influence of temperature increase on nucleation of the seeds in the first stage of the growth. Higher substrate temperatures lead to formation of larger seeds. Moreover, the nanowires are completely straight and are not needle-like at all.

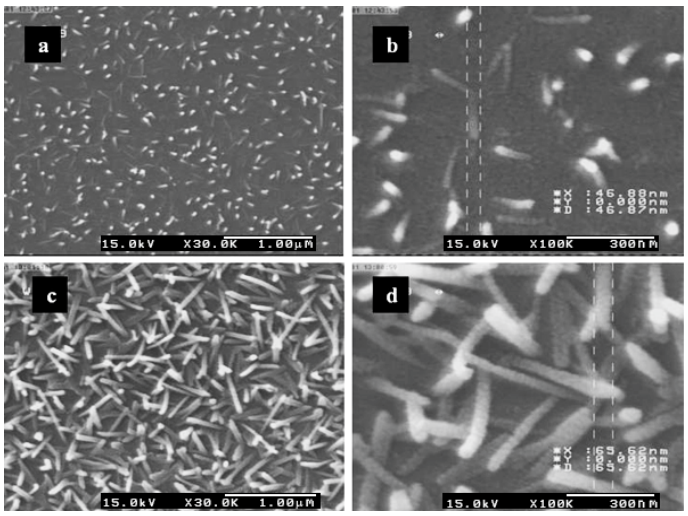

Figure 7. FESEM images of grown structures at 10^{-3} mbar pressure. Panels a and b are the images of structures on a 136 ^{o}C glass substrate placed at 28 cm from the 353 ^{o}C boat. Panels c and d are the images of grown structures on a 213 ^{o}C glass substrate placed at 24 cm from the 353 ^{o}C boat.

Figures 7a and 7b show the FESEM images of the structures synthesized on a 136 ^{o}C glass substrate placed at 33 cm from the 353 ^{o}C boat at 10^{-3} mbar. The grown nanowires have an average diameter of 50 nm, were most of them are almost perpendicular to the substrate surface due to lack of argon gas flow in the experiment. Images of nanostructures synthesized at the same pressure, on a glass substrate of 213 ^{o}C are indicated in Figures 7c and 7d. The nanowire with diameter of 65 nm can be clearly seen in the high magnification FESEM image. The considerable increase in the diameter of nanowires could be explained via nucleation process. When the substrate is closer to the boat, mostly an increase in the number of sites on the substrate surface is resulted that is thermodynamically suitable for nucleation and growth. So we observed a higher density of nanostructures in this case. Furthermore, the lack of gas flow in the furnace at 10^{-3} mbar, causes the evaporated Tellurium to have a higher concentration over the nearest substrates to the boat. Consequently, the final pattern is a dense distribution of nanowires that are almost perpendicular to the substrate.

The formation of the TeNWs can be explained through a vapor-solid (VS) growth mechanism. Generally, in the VS growth mechanism the morphology of the nanostructures is controlled by the degree of supersaturation, which itself is dependent on the evaporation temperature, deposition temperature,

www.SID.ir

Archive of SID

and the gas flow rate. To enable anisotropic growth to form whiskers or nanowires, the supersaturation ratio of the condensing species must be maintained below some critical value, above which two dimensional or even isotropic growth occurs. Thus, a low supersaturation ratio is required for anisotropic growth, whereas a medium supersaturation ratio leads to the growth of bulk crystals. At high supersaturation ratios, homogeneous nucleation in the vapor phase results in powder formation [32]. In the present case, the nanowires were formed through the vapor phase growth because of the low degree of supersaturation of the Tellurium vapor at temperatures which are much lower than the melting point of Tellurium.

Although the main interest of this paper is the growth of nanowires, but to find out the possible effect of changing the type of substrate, we repeated the experiment for the silicon (100) substrate. The results did not show a good growth for the nanowires in this case.

Figures 8a and 8b show FESEM images of the structures synthesized on a 146ºC silicon (100) substrate placed at 32 cm from the 353 ºC boat at 10^{-3} mbar. The grown nanostructures are needle-shaped nanowires or crystallites with tapered tips. In Figure 8b it can be seen that the broad base of the typical nanowire has a diameter of 59 nm. Increasing the substrate temperature resulted in considerable changes in shape and size of the nanostructures. As it is seen in Figures 8c and 8d the structures synthesized on a 235 ºC (100) silicon substrate placed at 21.5 cm from the 353 ºC boat at 10^{-3} mbar have mostly blade-shaped morphologies. It is observed that the diameter of the grown structure increased from about 59 nm in Figure 8b to about 347 nm in Figure 8d by increasing the substrate temperature by 89 ºC. Furthermore, the structures have not grown separately on the surface. They are joined together making a Y-shaped, T-shaped, or other similar shaped structures. Unlike the structures grown on glass substrates at 10^{-3} mbar pressure, the structures grown on silicon substrates are lying on the substrate. Figure 8e is a low magnification FESEM image of the same sample. It shows the dense distribution of the structures synthesized along a scratch on the silicon surface.

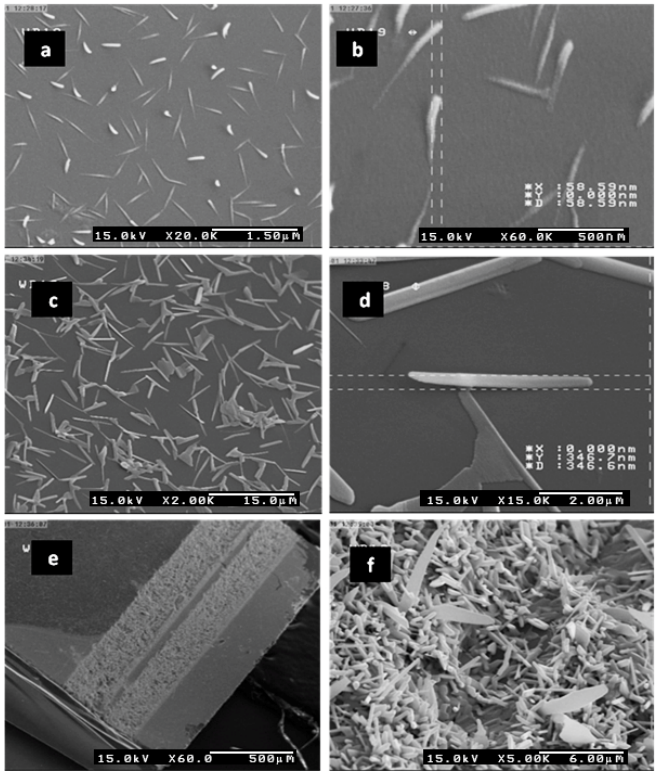

Figure 8. FESEM images of grown structures at 10^{-3} mbar pressure on silicon (100) substrate. Panels a and b show the images of structures grown on a 146 ºC substrate placed at 32 cm from the 353 ºC boat. Panels c and d are the images of structures grown on a 235 ºC silicon (100) substrate placed at 21.5 cm from the 353 ºC boat. Panel e is the low magnification image of grown structures along the scratched area of 235ºC (100) silicon substrate placed at 21.5 cm from the 353 ºC boat. Panel f is the high magnification image of the structures synthesized along the scratch.

It is clear from Figure 8f that the changes on the substrate surface results in the creation of a variety of structures such as rods, wires and blades with high densities in the area.

5 Conclusions

We have successfully fabricated crystalline TeNWs by a vapor phase approach. The noncatalytic and template-free vapor transport process has been employed to prepare TeNWs. The nanowires were synthesized on glass substrates with 136 ºC and 213 ºC temperatures at 10^{-3} mbar; 177 ºC, 186 ºC, and 196 ºC temperatures at 10^{-2} mbar; and 132 ºC and 185 ºC temperatures at 10^{-1} mbar pressure. The growth of these nanostructures has been understood on the basis of a Tellurium crystal structure and the vapor-solid growth mechanism. It was observed that under the

www.SID.ir

Archive of SID

controlled condition, the growth mechanism involved nucleation of spherical particles followed by the growth of structures in one dimension which was the result of anisotropic properties. Different structures were grown on the silicon (100) substrate at 146 °C and 235 °C temperatures. The role of the substrate type was observed by comparing the grown structures on glass and silicon substrates.

Acknowledgments

The financial support from the Academic Center of Education, Culture and Research, Tehran, Iran is acknowledged.

References

[1] R. R. Silva, H. A. G. Mejia, S. J. L. Ribeiro, L. K. Shrestha, K. Ariga, O. N. Oliveira Jr, V. R. Camargo, L. J. Q. Maia, C. B. Araújo, "Facile synthesis of Tellurium nanowires and study of their third-order nonlinear optical properties." Journal of the Brazilian Chemical Society, **28** (2017) 58.

[2] G. Wei, Y. Deng, Y. H. Lin, C. W. Nan, "Solvothermal synthesis of porous Tellurium nanotubes." Chemical Physics Letters, **372** (2003) 590.

[3] P. Mohanty, T. Kang, B. Kim, J. Park, "Synthesis of single crystalline Tellurium nanotubes with triangular and hexagonal cross sections." The Journal of Physical Chemistry B, **110** (2006) 791.

[4] V. Kumar, S. Sen, M. Sharma, K. P. Muthe, N. K. Gaur, S. K. Gupta, "Tellurium nano-structure based NO gas sensor." Journal of Nanoscience and Nanotechnology, **9** (2009) 5278.

[5] S. Sen, M. Sharma, V. Kumar, K. P. Muthe, P. V. Satyam, U. M. Bhatta, M. Roy, N. K. Gaur, S. K. Gupta, J. V. Yakhmi. "Chlorine gas sensors using one-dimensional Tellurium nanostructures." Talanta, **77** (2009) 1567.

[6] X. Y. Liu, M. S. Mo, X. Y. Chen, Y. T. Qian, "A rational redox route for the synthesis of Tellurium nanotubes." Inorganic Chemistry Communications, **7** (2004) 257.

[7] Z. Liu, Z. Hu, J. Liang, S. Li, Y. Yang, S. Peng, Y. Qian, "Size-controlled synthesis and growth mechanism of monodisperse Tellurium nanorods by a surfactant-assisted method." Langmuir, **20** (2004) 214.

[8] S. Ran, T. S. Glen, B. Li, T. Zheng, I. S. Choi, S. T. Boles, "Mechanical properties and piezoresistivity of Tellurium nanowires." The Journal of Physical Chemistry C, **123** (2019) 22578.

[9] P. K. Balguri, D. G. H. Samuel, D. B. Aditya, S. V. Bhaskar, U. Thumu, "Enhanced flexural strength of Tellurium nanowires/epoxy composites with the reinforcement effect of nanowires." Materials Science and Engineering, **310** (2018) 012157.

[10] C. Yan , T. Yu, C. Ji, X. Zeng, J. Lu, R. Sun, C. P. Wong, "3D interconnected high aspect ratio Tellurium nanowires in epoxy nanocomposites: serving as thermal conductive expressway." Journal of Applied Polymer Science, **135** (2018) 47054.

[11] Y. Wu, T. Guo, Y. Qiu, Y. Lin, Y. Yao, W. Lian, L. Lin, J. Song, H. Yang, "An inorganic prodrug, Tellurium nanowires with enhanced ROS generation and GSH depletion for selective cancer therapy." Chemical Science, **10** (2019) 7068.

[12] V. A. Berezovets, Y. A. Kumzerov, Y. A. Firsov, "Electron Transport in Tellurium Nanowires." Physics of the Solid State, **60** (2018) 256.

[13] Q. Wang, G. D. Li, Y. L. Liu, S. Xu, K. J. Wang, J. S. Chen, "Fabrication and growth mechanism of selenium and Tellurium nanobelts through a vacuum vapor deposition route." The Journal of Physical Chemistry C, **111** (2007) 12926.

[14] C. Me´traux, B. Grobe´ty, "Tellurium nanotubes and nanorods synthesized by physical vapor deposition." Journal of Materials Research, **19** (2004) 2159.

[15] A. W. Zhao, C. H. Ye, "Tellurium nanowire arrays synthesized by electrochemical and electrophoretic deposition." Journal of Materials Research, **18** (2003) 2318.

[16] B. Mayers, Y. Xia, "One-dimensional nanostructures of trigonal Tellurium with various morphologies can be synthesized using a solution-phase approach." Journal of Materials Chemistry, **12** (2002) 1875.

[17] Z. Liu, Z. Hu, Q. Xie, B. Yang, J. Wu, Y. Qian, " Surfactant-assisted growth of uniform nanorods of crystalline Tellurium." Journal of Materials Chemistry, **13** (2002) 159.

[18] M. Mo, J. Zeng, X. Liu, W. Yu, S. Zhang, Y. Quian, "Controlled hydrothermal synthesis of thin single-crystal Tellurium nanobelts and nanotubes." Advanced Materials, **14** (2002) 1658.

[19] Z. Wang, L. Wang, J. Huang, H. Wang, L. Pan, X. Wei, "Formation of single-crystal Tellurium nanowires and nanotubes via hydrothermal recrystallization and their gas sensing properties at

www.SID.ir

Archive of SID

room temperature." Journal of Materials Chemistry, **20** (2010) 2457.

[20] F. Liang, H. Qian, "Synthesis of Tellurium nanowires and their transport property." Materials Chemistry and Physics, **113** (2009) 523.

[21] A. V. Crua, D. Medina, T. J. Webster, J. L. C. Diaz, J. M. G. Martin, "Green synthesis of a synergetic structure of Tellurium nanowires and metallic nanoparticles for biomedical applications." AIChE Annual Meeting, (2019)

[22] Y. J. Zhu, X. Hu. "Tellurium nanorods and nanowires prepared by the microwave-polyol method." Chemistry Letters, **33** (2004) 760.

[23] T. Vasileiadis, V. Dracopoulos, M. Kollia, S. N. Yannopoulos, "Laser-assisted growth of t-Te nanotubes and their controlled photo-induced unzipping to ultrathin core-Te/ sheath-TeO_2 nanowires." Scientific Reports, **3** (2013) 1209 .

[24] M. Hunyadi, Z. Gácsi, I. Csarnovics, L. Csige, A. Csik, L. Daróczi, R. Huszánk, Z. Szűcs, "Enhanced growth of Tellurium nanowires under conditions of macromolecular crowding." Physical Chemistry Chemical Physics, **19** (2017) 16477.

[25] Y. Li, W. Zhao, X. Mu, X. Liu, D. He, W. Zhu, Q. Zhang, "Synthesis and characterization of high-purity Tellurium nanowires via self-seed-assisted growth approach." Journal of Electronic Materials, **45** (2016) 1661.

[26] U. K. Gautam, C.N.R. Rao. "Controlled synthesis of crystalline tellurium nanorods, nanowires ,nanobelts and related structures by a self-seeding solution process." J. Materials Chemistry, **16** (2004) 2530.

[27] S. Sen, U. M. Bhatta, V. Kumar, K. P. Muthe, "Synthesis of Tellurium nanostructures by physical vapor deposition and their growth mechanism." Crystal Growth & Design, **8** (2008) 238.

[28] X. L. Li, G. h. Cao, C. m. Feng, Y. d. Li,"Synthesis and magnetoresistance measurement of Tellurium microtubes." Journal of Materials Chemistry, **14** (2004) 244.

[29] P. Mohanty, J. Park, B. Kim. "Large scale synthesis of highly pure single crystalline Tellurium nanowires by thermal evaporation method." Journal of Nanoscience and Nanotechnology, **6** (2006) 3380.

[30] K. R. Sapkota, P. Lu, D. L. Medlin, G. T. Wang, "High temperature synthesis and characterization of ultrathin Tellurium nanostructures." APL Materials, **7** (2019) 081103.

[31] N. Parsafar, A. Ebrahimzad, "The effect of substrate temperature on fabrication of one-dimensional nanostructures of Tellurium." International Journal of Nano Dimension, **2** (2012) 177.

[32] Y. J. Hsu, S. Y. Lu, "Vapor-solid growth of Sn nanowires: growth mechanism and superconductivity." The Journal of Physical Chemistry B, **109** (2005) 4398.

www.SID.ir